COMMUN. STATIST.—STOCHASTIC MODELS, 12(2), 199-214 (1996)

Statistical Models of Random Polyhedra

I.S. MOLCHANOV
Centrum voor Wiskunde en Informatica
P.O.Box 94079, 1090 GB Amsterdam, The Netherlands

D. STOYAN
TU Bergakademie Freiberg, Institut für Stochastik
D-09596 Freiberg, Germany

Abstract The paper discusses problems which appear in statistics of random polyhedra. Several parametric models of random polyhedra are considered. Particular attention is paid to the model of convex-stable compact random sets, which appear as weak limits of normalized convex hulls of systems of random points. It depends on two parameters only, but nevertheless provides sufficient flexibility of shape, and allows computations of several motion-invariant characteristics. The application of the model is demonstrated for real samples of particles.

Keywords: Extremes, random compact set, random polygon, random polyhedron, shape, convex hull, area-perimeter ratio, compacity.

This research was partially supported by the Alexander von Humboldt-Stiftung, Bonn, Germany. The first author was supported also by the Dutch Organization for Advancement of Pure Researches (NWO).

1. INTRODUCTION

This paper discusses some models and related statistical methods for random convex polygons. Statistical studies of compact sets are difficult due to the lack of models which allow evaluations and provide sufficiently variable shapes. Other problems appear, since for an observer typically positions and/or orientations of the set-valued observations are unknown. This means that samples of *figures* rather than samples of sets are considered. (A figure is an equivalence class containing all sets equal up to Euclidean motions.) Indeed, in the statistical analysis of sand grains or powder particles the question of location and orientation does not make sense at all.

Similar problems are treated in the statistical theory of shape developed by Kendall [15] and Bookstein [3]. There a figure is represented by a finite collection of "specific" points, called *landmarks*. Then motion- and scale-invariant statistics of these point configurations are considered, see [3, 27, 28]. However, this approach ignores the initial model of a random set, and in particle statistics it is not natural to define landmarks.

We use an approach based on motion-invariant characteristics. This is also the approach used by engineers in applied studies, see [13]. To eliminate size effects and emphasize the shape distribution we argue for using of *shape-ratios* (normalized measurements) which are also invariant with respect to scale transformations. For example, the area is not scale-invariant, but the area divided by the square of perimeter is scale-invariant.

Random polyhedra (or polygons in the planar case) form a simple class of random compact sets in the Euclidean space. By now there are very few *parametric* models of random polyhedra. Some of them are mentioned in [28], while Hawkins [13] used only a descriptive approach and did not at all consider models or distributions. The known standard models are obtained as typical polyhedra in tessellations. Unfortunately, these models depend on one parameter only, and more sophisticated models of this type are too complicated for computations of their invariant characteristics. In this paper we suggest an alternative, namely a simple two-parametric model based on weak limits of convex hulls of random points. This model allows numerical computations of several important shape and size parameters, and at the same time it gives polyhedra of sufficiently variable shapes. The first parameter of the model controls the polyhedron's size, while the second determines its shape.

The paper is organized as follows. Section 2 recalls some generalities on random compact sets. Section 3 presents several parametric models of random polyhedra. Distributional characteristics of so-called convex-stable polyhedra are treated in Section 4. Simulation results for some shape characteristics are given in Section 5. Finally, in Section 6 three samples of nearly polyhedral particles are analyzed.

2. RANDOM COMPACT SETS

A *random compact set* X is a random element in the space $\mathcal{K}$ of all non-empty compact subsets of the Euclidean space $\mathbf{R}^d$. The measurability condition ensures that $\{X \cap K \neq \emptyset\}$ is a random event for each $K \in \mathcal{K}$. The famous Choquet theorem [16] yields that the distribution of a random compact set is determined by the values of the *capacity* (or *hitting*) functional $\mathbf{P}\{X \cap K \neq \emptyset\}$ for K running through $\mathcal{K}$. Also the *containment* functional $\mathbf{P}\{X \subset K\}$, $K \in \mathcal{K}$, suffices to determine uniquely the distribution of a random compact set X. Moreover, if X is a *convex compact* random set, then its distribution is determined by the containment functional with K running through the smaller class of *convex* compacts, see [19, 29].

A random set X is said to be *isotropic* if its distribution is invariant with respect to non-random rotations around the origin.

The statistical analysis of random sets often begins with a study of some numerical characteristics. In practice, an observer uses several values of functionals $f_1(X_i), \dots, f_m(X_i)$ for each observation X_i of a random compact set X. Then the problem can be reduced to observations of a random vector with the subsequent use of techniques of multivariate statistics. However, the corresponding distributions are very difficult to compute and to handle.

For convex compact random sets it is natural to work with the values $f_j(X) = h(X, u_j)$, $1 \leq j \leq m$, of the support function

$$h(X, u) = \sup\{\langle u, x\rangle \colon x \in X\}$$

of X at different points $u_1, \dots, u_m$ of the unit sphere $\mathbf{S}^{d-1}$. Here $\langle u, x\rangle$ denotes the scalar product in $\mathbf{R}^d$. Of course, these values do not allow one to retrieve the shape of X.

The support function $h(X, u)$ is not invariant with respect to motions of X. However, if the location (orientation) of X is not known, then all measurements $f_j(X)$ should be invariant with respect to shifts (rotations) of X. Examples of such measurements are: area (denoted by $\mathsf{A}(X)$), volume, perimeter ($\mathsf{U}(X)$), number of connected components, surface area or other geometric functionals and shape-ratios, see [13, 22, 28]. In the planar case we will often use the *compacity* or area-perimeter ratio of X given by

$$\mathsf{C}(X) = \frac{4\pi \mathsf{A}(X)}{\mathsf{U}(X)^2}\,. \tag{2.1}$$

Note that $0 \leq \mathsf{C}(X) \leq 1$, and $\mathsf{C}(X) = 1$ if and only if X is a disk. For other shape ratios see [28] and [13]. The computational techniques for real data are discussed in [21, 22, 26].

3. PARAMETRIC MODELS

In this section some parametric models of random compact polyhedra (polygons in the planar case) are considered. All examples are centered with respect to the origin. Nevertheless, these random polygons can serve as representatives of the corresponding (non-centered) random figures.

3.1. Poisson polyhedron. This is the "typical" random polyhedron X generated by the stationary and isotropic Poisson hyperplane tessellation of intensity λ, see [16, 27, 28]. To obtain random sets, all polyhedra generated by the family of hyperplanes are shifted in such a way that their centres of gravity lie on the origin. These shifted polyhedra are interpreted as realizations of the "typical" random polyhedron X. The moments of its main geometric characteristics were given in [16], see also [17], [27, p.271].

3.2. Poisson-Dirichlet polyhedron. Let us consider the Dirichlet (or Voronoi) mosaic generated by the stationary Poisson point process of intensity λ. For each point x_i we construct the open set containing all points of the plane whose distance to x_i is less than the distances to other points. If shifted by x_i, the closures of these sets give realizations of the so-called Poisson-Dirichlet polyhedron, see [28].

Several important numerical parameters of the Poisson polygon and the Poisson-Dirichlet polygon (in the planar case, $d = 2$) are given in Table 3.1. These values are taken from [28]. Note that the second moments for the Poisson-Dirichlet polygon are obtained only by simulation or numerical integration. The functionals in the last two columns are motion- and scale-invariant. Also the number of vertices is a motion- and scale-invariant functional, but we do not recommend its practical use, since small defects on boundaries of real figures can produce too many vertices.

The distributions of both Poisson polygon and Poisson-Dirichlet polygon depend on one parameter only, the corresponding intensity parameter λ (having different meanings for both models). Moreover, both models can be obtained by scale transforms from the corresponding sets with $\lambda = 1$. For example, the Poisson-Dirichlet polygon X has the same distribution as $\lambda^{-1/2}X_1$, where X_1 is the Poisson-Dirichlet polygon obtained by the point process with unit intensity. Thus, λ affects only size characteristics of the corresponding random sets, while their scale-invariant characteristics, e.g., the mean value of *compacity*, $\mathsf{C}(X)$, do not depend on λ. For the Poisson-Dirichlet polygon 1000 simulations gave the result $\mathbf{E}\mathsf{C}(X) \approx 0.72$ with the standard deviation $\sigma_{\mathsf{C}(X)} = 0.10$.

3.3. Convex hulls of a finite number of points (finite convex hulls). Another model of a random isotropic polyhedron is the convex hull of N independent points uniformly distributed within the ball $B_r(o)$ of radius r centered at the origin, see [28]. For given N, the containment functional of this poly-

Table 3.1:
Numerical characteristics of the Poisson and the Poisson-Dirichlet polygons.

	$\mathrm{EA}(X)$	$\mathrm{EU}(X)$	$\mathrm{E}(\mathrm{U}(X)^2)$	$\frac{\sigma_{\mathrm{U}(X)}}{\mathrm{EU}(X)}$	$\frac{\mathrm{EU}(X)}{\sqrt{\mathrm{EA}(X)}}$
Poisson polygon	$4\lambda^{-2}/\pi$	$4\lambda^{-1}$	$(2\pi^2+8)\lambda^{-2}$	$\sqrt{2\pi^2-8}/4$ ≈ 0.857	$2\sqrt{\pi}$ ≈ 3.545
Poisson-Dirichlet polygon	λ^{-1}	$4\lambda^{-1/2}$	$\approx 16.947\lambda^{-1}$	≈ 0.243	4

hedron X is given by

$$\mathrm{P}\{X \subset K\} = \left(\frac{\mu_d(K)}{b_d r^d}\right)^N, \quad K \subset B_r(o),$$

where K is a convex subset of $B_r(o)$, μ_d is the Lebesgue measure in $\mathbf{R}^d$ and b_d is the volume of the unit ball in $\mathbf{R}^d$. However, further exact distributional characteristics are not so easy to find; mostly only asymptotic properties for large n can be investigated, see [6, 7, 14, 23, 25]. The values of r and N are the two model parameters. The radius of the ball affects the size of polyhedra, while N determines their shapes. Convex hulls of random balls were considered in [1, 11].

3.4. Convex-stable sets. Convex-stable sets (more precisely, strictly convex-stable in the terminology of [18, 19]) appear as weak limits of scaled convex hulls

$$a_n^{-1}\mathrm{conv}(Z_1 \cup \cdots \cup Z_n)$$

of iid random compact sets $Z_1, Z_2, \ldots$ having a regularly varying distribution in a certain sense, see [19] for a detailed discussion. The $a_n > 0$, $n \geq 1$, are positive constants such that $a_n \to \infty$ as $n \to \infty$.

We will deal only with the simplest model where X is the weak limit of convex hulls of random singletons ($Z_i = \{\xi_i\}$). This case was studied also in [2, 4, 5, 8]. However, until now the corresponding convex hulls have not been used as models of convex polyhedra.

In order to obtain non-degenerate limit distributions, the probability density f of the ξ_i's must be *regular varying at infinity*, i.e., for any vector $e \neq o$,

$$\lim_{t\to\infty} \frac{f(tu_t)}{f(te)} = \phi(u) \neq 0 \text{ or } \infty\,, \tag{3.1}$$

for $u_t \to u \neq o$ as $t \to \infty$, see [12, 19, 24]. Then ϕ is continuous and homogeneous, that is,

$$\phi(su) = s^{-\alpha-d}\phi(u), \quad s > 0\,, \quad u \in \mathbf{R}^d\,. \tag{3.2}$$

Furthermore, the function $L(u) = f(u)/\phi(u)$ is slowly varying, i.e., it satisfies (3.1) with the right side equal to 1. If $\alpha > 0$ in (3.2) then, for $a_n = \sup\{t\colon\ t^{-\alpha}L(te) \geq n^{-1}\}$, the convex hulls

$$a_n^{-1}\mathrm{conv}(\xi_1, \ldots, \xi_n) \tag{3.3}$$

converge weakly (in distribution) as $n \to \infty$ to the convex-stable random set X with the containment functional

$$\mathbf{P}\{X \subset K\} = \exp\left\{-\int_{K^c} \phi(u)du\right\}\,, \tag{3.4}$$

where K^c is the complement of K, see [18, 19]. Note that X is isotropic if and only if $\phi(u)$ depends on the norm $\|u\|$ only.

The limiting random set X can be equivalently represented as the convex hull of a *scale invariant Poisson point process*, see [9, p.325]. This is a non-stationary Poisson process whose intensity function satisfies (3.2). Then (3.4) follows directly from the Poisson property. Unfortunately, it is not easy to simulate such a point process directly, since its intensity measure is infinite in the origin.

To satisfy (3.1), the density f must have power tails. In the isotropic case we will use the density

$$f(u) = \frac{c}{c_1 + \|u\|^{\alpha+d}}\,, \quad u \in \mathbf{R}^d\,, \tag{3.5}$$

for some $\alpha > 0$ and suitable positive constants c and c_1. The constant c is a scaling parameter, while the normalizing parameter c_1 is chosen in such a way that f is a probability density function. Then (3.1) is valid, $a_n \sim n^{1/\alpha}$ as $n \to \infty$, and, for $\|e\|^{\alpha+d} = c$, (3.1) yields $\phi(u) = c\|u\|^{-\alpha-d}$. Thus, for $a_n = n^{1/\alpha}$, the random set (3.3) converges weakly to the isotropic convex-stable set X with the containment functional (3.4).

Thus, the model has two parameters: the *size parameter* c and the *shape parameter* α. The choice of a *positive* α implies that X is almost surely a compact convex polyhedron, see [10].

A possible engineering motivation for the model of convex-stable polyhedra may be the following. Suppose that particles were obtained as the result of high pressures applied to dust clouds. These high pressures correspond to

scale transformations (3.3) of the clouds with parameter $a_n \to \infty$. Then the shape of the limiting convex hull is determined only by those elementary dust particles which are very far from the origin. If the distribution of dust particles has a regular varying density, then the limit is non-degenerate and corresponds to a convex-stable polyhedron.

4. NUMERICAL CHARACTERISTICS OF CONVEX-STABLE RANDOM POLYHEDRA

Here we give some mean values of numerical parameters of a convex-stable random polyhedron X with containment functional (3.4). We consider only the isotropic case for which the formulae are simpler.

4.1. Support function. The distribution of the support function of X is given by

$$\mathbf{P}\{h(X,u) < x\} = \mathbf{P}\{X \subset (H_u(x))^c\} = \exp\left\{-\int\limits_{H_u(x)} \phi(w)dw\right\},$$

where $\phi(w) = c\|w\|^{-\alpha-d}$, and $H_u(x) = \{v\colon \langle u,v\rangle \geq x\}$, $x > 0$. Integration gives the result

$$\mathbf{P}\{h(X,u) < x\} = \exp\left\{-x^{-\alpha}a(\alpha)\right\},$$

where

$$a(\alpha) = \alpha^{-1} \int\limits_{\|v\|=1,\,\langle u,v\rangle \geq 0} \phi(v)\langle u,v\rangle^{\alpha} dv\,.$$

The integral does not depend on $u \in \mathbf{S}^{d-1}$, and the integration is taken with respect to the surface area measure on $\mathbf{S}^{d-1}$. Thus,

$$\mathbf{E}h(X,u) = \Gamma(1-\alpha^{-1})a(\alpha)^{1/\alpha}, \quad u \in \mathbf{S}^{d-1}, \tag{4.1}$$

where Γ is the gamma-function. The expectation is finite if and only if $\alpha > 1$, see also [4].

The covariance of the support function of X can be computed by means of the formula

$$\mathbf{P}\{h(X,u) < x, h(X,v) < y\} = \exp\left\{-\int\limits_{H_u(x)\cup H_v(y)} \phi(w)dw\right\} \tag{4.2}$$

for the joint distribution function of $h(X,u)$ and $h(X,v)$. Note that the second moment of the support function is finite only if $\alpha > 2$. Then

$$\mathbf{E}h(X,u)^2 = a(\alpha)^{2/\alpha}\Gamma(1-2\alpha^{-1})\,.$$

Furthermore, (4.2) implies the independence of $h(X,u)$ and $h(X,-u)$.

The results above yield the first two moments of the width function $b(X,u) = h(X,u) + h(X,-u)$:

$$\mathbf{E}b(X,u) = \mathbf{E}h(X,u) + \mathbf{E}h(X,-u)\,, \tag{4.3}$$

$$\mathbf{E}b(X,u)^2 = \mathbf{E}h(X,u)^2 + 2\mathbf{E}h(X,u)\mathbf{E}h(X,-u) + \mathbf{E}h(X,-u)^2\,. \tag{4.4}$$

Note that the width function is translation-invariant, but not rotation-invariant.

4.2. Planar case. If $d = 2$ and the density f is rotation-invariant, then $\phi(u) = c\|u\|^{-\alpha-2}$. Therefore,

$$a(\alpha) = \frac{c}{\alpha}\int_{-\pi/2}^{\pi/2}(\cos\beta)^\alpha d\beta = \frac{c\sqrt{\pi}}{\alpha}\,\frac{\Gamma(\frac{1}{2}(\alpha+1))}{\Gamma(1+\frac{\alpha}{2})}\,. \tag{4.5}$$

The expected values of the geometric functionals of X in the planar case are given in [4, 8]. In our notations

$$\mathbf{E}\mathsf{U}(X) = 2\pi\Gamma(1-\alpha^{-1})a(\alpha)^{1/\alpha} \tag{4.6}$$

and

$$\mathbf{E}\mathsf{A}(X) = \frac{\alpha\pi}{\alpha-1}\Gamma(2-2\alpha^{-1})a(\alpha)^{2/\alpha}\,. \tag{4.7}$$

It follows from (4.6) and (4.7) that

$$\mathbf{E}\mathsf{U}(X)/\sqrt{\mathbf{E}\mathsf{A}(X)} = 2\pi\Gamma(1-\alpha^{-1})\left(\frac{\pi\alpha}{\alpha-1}\Gamma(2-2\alpha^{-1})\right)^{-1/2}\,. \tag{4.8}$$

4.3. Expected mean width and mean square width. The two parameters in the isotropic case, c and α, can be determined by the method of moments. However, the second moments of motion-invariant characteristics are not known theoretically. In the planar case it is possible to find shape parameter α from (4.8) or (4.6) and (4.7) using the mean area and the mean perimeter of X. As soon as α is found, c can be estimated by means of (4.5) and (4.6) or (4.7).

Unfortunately, mean volume and mean surface area are not known theoretically for higher dimensions. Therefore, two other characteristics are considered. The first is the mean width

$$\mathsf{M}(X) = \frac{1}{\omega_{d-1}}\int_{\mathbf{S}^{d-1}} b(X,u)du$$

of X, where ω_{d-1} is the surface area of the unit sphere in $\mathbf{R}^d$. In the planar case $\mathsf{M}(X) = \mathsf{U}(X)/\pi$. In general, (4.1) and (4.3) yield

$$\mathbf{E}\mathsf{M}(X) = 2a(\alpha)^{1/\alpha}\Gamma(1-\alpha^{-1})\,.$$

Instead of the second moment of $\mathsf{M}(X)$ (which is difficult to compute) we consider the expectation of

$$\mathsf{M}_2(X) = \frac{1}{\omega_{d-1}} \int\limits_{\mathbf{S}^{d-1}} b(X,u)^2 du\,.$$

Formula (4.4) yields

$$\mathbf{E}\mathsf{M}_2(X) = 2\left[\Gamma(1-2\alpha^{-1}) + \Gamma(1-\alpha^{-1})^2\right] a(\alpha)^{2/\alpha}\,,$$

whence

$$2\frac{\mathbf{E}\mathsf{M}_2(X)}{(\mathbf{E}\mathsf{M}(X))^2} = \frac{\Gamma(1-2\alpha^{-1})}{\Gamma(1-\alpha^{-1})^2} + 1\,. \tag{4.9}$$

Note that this equation remains the same for any d.

4.4. Three-dimensional convex-stable sets and their projections. If X is an isotropic convex-stable polyhedron in $\mathbf{R}^d$, then its lower-dimensional projections are distributed as isotropic convex-stable polyhedra in the corresponding lower-dimensional spaces. For instance, suppose that X is a convex-stable isotropic polyhedron in $\mathbf{R}^3$ with parameters c and α. Let Y be its planar projection. Then, for any planar convex set K,

$$\mathbf{P}\{Y \subset K\} = \mathbf{P}\{X \subset K'\} = \exp\left\{-\int\limits_{(K')^c} c\|u\|^{-\alpha-3} du\right\},$$

where K' is the cylinder built on K. Let v be a unit vector orthogonal to the projection plane. Then

$$\begin{aligned}\mathbf{P}\{Y \subset K\} &= \exp\left\{-\int\limits_{K^c}\int\limits_{-\infty}^{+\infty} c\|u+tv\|^{-\alpha-3} du dt\right\} \\ &= \exp\left\{-c\int\limits_{K^c}\|u\|^{-\alpha-2} du \int\limits_{-\infty}^{+\infty}(1+t^2)^{-(\alpha+3)/2} dt\right\}.\end{aligned}$$

This immediately yields that Y is a convex-stable isotropic polygon with the same shape parameter α as X and the size parameter

$$c' = c\int\limits_{-\infty}^{+\infty}(1+t^2)^{-(\alpha+3)/2} dt = c\sqrt{\pi}\,\frac{\Gamma(\alpha/2+1)}{\Gamma((\alpha+3)/2)}\,. \tag{4.10}$$

Therefore, it is possible to estimate parameters of 3-dimensional convex-stable polyhedra by their planar projections.

Other models of random polyhedra in Section 3 do not possess such a property. For example, if X is a finite convex hull of N points uniformly

distributed within $B_R(o)$, then its projection can be no longer interpreted as the convex hull of points uniformly distributed within a $(d-1)$-dimensional ball (even for different numbers of points and the ball's radii). Furthermore, the Poisson polyhedron X in $\mathbf{R}^3$ is not projection-invariant, since for its planar projection, X', $\mathbf{E}A(X')^2/(\mathbf{E}A(X'))^2 = 4\pi^2/9$, while this value for the two-dimensional Poisson polygon is $\pi^2/2$, see [16, pp.180-181].

5. SIMULATION OF PLANAR ISOTROPIC CONVEX-STABLE SETS

Some mean shape characteristics of convex-stable polygons can be computed using the formulae of Section 4. For many other the only way of obtaining numerical values is simulation. This is similar to the case of Poisson-Dirichlet polygons, see [20, 28].

Below some simulation results for isotropic convex-stable polygons in $\mathbf{R}^2$ with different parameters α are given. We explain the simulation in order to help to understand the model of convex-stable sets.

Each realization of a random convex-stable polygon with given α is simulated by scaling of the convex hull of $n = 1000$ independent identically distributed random points $\xi_1, \dots, \xi_{1000}$ having the regularly varying isotropic density (3.5) with tail proportional to $\|x\|^{-2-\alpha}$, $\alpha > 1$. In polar coordinates ξ_i is expressed as $\xi_i = \upsilon_i \eta_i$, where υ_i is uniformly distributed on the unit circle and η_i is a positive random variable. If η_i has the density

$$p(r) = \frac{cr}{1 + r^{2+\alpha}}, \quad r > 0, \tag{5.1}$$

then the density of ξ_i is given by $f(x) = p(\|x\|)/(2\pi\|x\|)$. Thus, $f(x)$ has the right tail rate $\|x\|^{-2-\alpha}$, whence the corresponding convex-stable polygon X has the shape parameter α and the size parameter

$$c = \left(\int_0^\infty \frac{r\,dr}{1 + r^{2+\alpha}} \right)^{-1} = \frac{2+\alpha}{\pi} \sin \frac{2\pi}{2+\alpha}.$$

The random variables η_i, $i \geq 1$, are simulated as follows.

1. Put $\zeta = \tan \frac{\pi\vartheta}{2}$ for ϑ uniformly distributed on $[0, 1]$. The random variable ζ has then a Cauchy distribution with density

$$g(r) = 2/(\pi(1 + r^2)), \quad r \geq 0. \tag{5.2}$$

(Note that $p_0(r) = p(r)(c\pi)^{-1} = \pi^{-1} r/(1 + r^{2+\alpha}) \leq g(r)$ for all $r \geq 0$.)

2. Simulate a random variable τ uniformly distributed in $[0, g(\zeta)]$.

3. If $p_0(\zeta) \geq \tau$, then accept the value of ζ as the simulated value of η_i, i.e. put $\eta_i = \zeta$. Otherwise repeat Step 1.

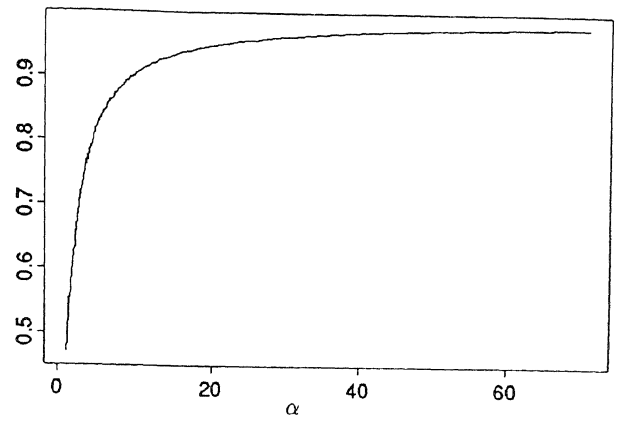

Figure 5.1:
The mean compacity $\mathrm{EC}(X)$ as a function of α.

The density of ξ_i has the form (3.5). Thus, the normalizing parameter in (3.3) can be chosen as $a_n = n^{1/\alpha}$. Each realization of X was simulated by taking the convex hull of $n = 1000$ i.i.d. points, whence

$$X = 1000^{-1/\alpha}\mathrm{conv}(\xi_1, \ldots, \xi_{1000}).$$

The random set X was simulated 1000 times. Figure 5.1 shows the graph of the mean compacity as a function of α. Table 5.1 gives several simulation results for the standard deviation of the compacity.

Note that if X has parameters c and α, then βX has parameters $c\beta^\alpha$ and α. Thus, convex-stable polygons with different size parameters can be obtained by scale transformations of the sample with a fixed c. However, we will use only scale-invariant characteristics, so simulations for one c suffice for our purposes.

Table 5.1:
Standard deviations of compacity for several values of α.

α	2.0	3.0	4.0	5.0	6.0	8.0	10.0	15.0
$\sigma_{\mathrm{C}(X)}$	0.167	0.119	0.093	0.075	0.062	0.047	0.033	0.022

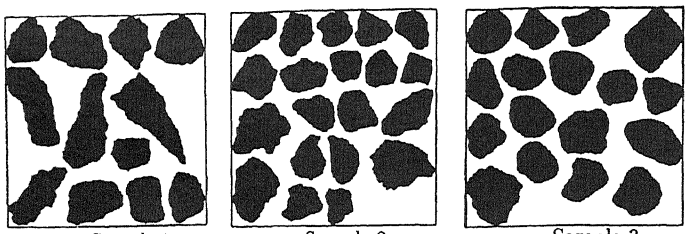

Figure 6.1:

Several planar projections of particles from three samples of sand grains analyzed by E.Pirard.

6. METHOD OF MOMENTS FOR INVARIANT STATISTICS

Let us consider three samples of sand particles, which were first analyzed by E.Pirard [21, 22]. Figure 6.1 gives planar projections of some specimens from each sample. The particles are not convex, but the deviations from convexity are small. We try to find a model of random convex polygons with shape and size characteristics similar to those of the samples.

The samples parameters are given in Tables 6.1 and 6.2. The empirical means of area, perimeter, compacity etc. are denoted by $\hat{m}_{\mathsf{A}}$, $\hat{m}_{\mathsf{U}}$, $\hat{m}_{\mathsf{C}}$ etc. respectively, and estimates of their standard deviations by $\hat{\sigma}$ with the corresponding subscripts. Note that Pirard estimated the perimeters of particles by averaging their three Feret diameters with respect to three main directions on a hexagonal lattice, see [26, p. 222] and [21, 22]. We used these values for evaluating $\mathsf{M}_2(X)$ by averaging the squares of these three directional diameters, while values of $\mathsf{M}(X)$ were estimated as arithmetic averages of the three diameters.

Comparison of the values given in Table 3.1 for Poisson polygon and Poisson-Dirichlet polygon with the empirical values of $\hat{m}_{\mathsf{U}}/\hat{m}_{\mathsf{A}}^{1/2}$ and $\hat{\sigma}_{\mathsf{U}}/\hat{m}_{\mathsf{U}}$ given in Table 6.2 suggests that for Pirard's particles the hypothesis of Poisson-Dirichlet polygons is more plausible than the hypothesis of Poisson polygons. However, the comparison of the empirical mean value of compacity with the theoretical value for Poisson-Dirichlet polygon throws doubts also on the first hypothesis. It was definitely rejected by a comparison of compacity *distributions*.

Thus the two classical polygon models turned out to be inappropriate. Therefore, we tried the model of convex-stable polygons. We applied the method of moments to estimate the shape parameter α. There are two possible methods. The first method is based on the empirical normalized perimeter from the second column of Table 6.2 and formula (4.8) and the second one uses

Table 6.1:
Empirical translation-invariant characteristics of particles.

number of sample	sample size	$\hat{m}_{\mathsf{A}}$ ($\times 10^5$)	$\hat{\sigma}_{\mathsf{A}}$ ($\times 10^4$)	$\hat{m}_{\mathsf{U}}$ ($\times 10^3$)	$\hat{\sigma}_{\mathsf{U}}$ ($\times 10^2$)	$\hat{m}_{\mathsf{M}_2}$ ($\times 10^4$)	$\hat{\sigma}_{\mathsf{M}_2}$ ($\times 10^3$)
1	203	1.74	5.05	1.66	2.69	2.22	7.61
2	203	1.26	3.40	1.41	2.15	1.60	4.98
3	183	1.29	3.23	1.34	1.72	1.43	3.76

Table 6.2:
Scale-invariant empirical characteristics.

number of sample	$\hat{m}_{\mathsf{U}}/\hat{m}_{\mathsf{A}}^{1/2}$	$\hat{\sigma}_{\mathsf{U}}/\hat{m}_{\mathsf{U}}$	$\hat{m}_{\mathsf{C}}$	$\hat{\sigma}_{\mathsf{C}}$	$2\hat{m}_{\mathsf{M}_2}/\hat{m}_{\mathsf{M}}^2$
1	3.9676	0.1624	0.7900	0.068	2.0907
2	3.9880	0.1521	0.7838	0.077	2.0708
3	3.7279	0.1281	0.8953	0.047	2.0570

formula (4.9) and values of M and M_2. The obtained estimates $\hat{\alpha}$ are given in Table 6.3.

We observe large differences in the second and the third columns of Table 6.3 and conclude that for the first two samples the range of α is from 3.5 to 6.0. Further we estimate α by comparisons of compacity distributions. For the first two samples we took the range of α from 3.5 to 6.0 with step 0.1, and used the Kolmogorov-Smirnov test to compare the distributions of compacity for particles and simulated polygons. The data from the third sample were treated in a similar way. The values of α with the highest significance levels and the corresponding significance levels are shown in the two last columns of Table 6.3. We see that the moment method based on (4.8) gives results close to those obtained by comparison of compacity distributions. Unfortunately, the

Table 6.3:
Estimates of α.

number of sample	$\hat{\alpha}$ based on (4.8)	$\hat{\alpha}$ based on (4.9)	$\hat{\alpha}$ based on $\hat{m}_C$	confidence levels
1	4.0	5.1	3.9	0.066
2	4.2	5.7	3.7	0.12
3	9.8	6.2	9.1	0.045

estimates obtained by using (4.9) are not satisfactory. This may be explained by the large empirical variances of the values of M_2, as shown in Table 6.1. Therefore, the method based on (4.9) requires larger samples and, perhaps, also the measurement of the width function (diameters) in more directions.

The value of the size parameter c can be estimated by substituting the true mean perimeter into (4.6) and using (4.5). For example, if the estimate $\hat{\alpha} = 3.7$ for the second sample is taken, then $\hat{c} = 6.68 \cdot 10^8$. Assuming that the original three-dimensional particles are distributed as convex-stable polyhedra, we can conclude from (4.10) that three-dimensional polyhedra corresponding to the second sample have the size parameter $7.29 \cdot 10^8$ and the shape parameter 3.7.

Finally, we try the model of finite convex hulls. Since theoretical values of the compacity for this model are not known, we used simulation series of 1000 experiments to determine the compacity for each number N of points from 3 to 60. From this we found those values of N which give mean compacities close to those given in Table 6.2. Then we used the Kolmogorov-Smirnov test to compare the simulated samples of compacities with the empirical ones. For the first sample the highest significance level (0.60) is achieved for $N = 16$. Thus, for the first sample, the finite convex hulls model gives a good coincidence of compacity distributions. For the second sample and all N the significance levels are small (the highest is $6.1 \cdot 10^{-3}$ for $N = 15$). For the third sample all significance levels are less than 10^{-4}.

Acknowledgements

The authors thank E.Pirard for providing his data sets and kind explanations. They are also grateful to U.Lorz for computing by simulation the mean shape

parameters of the Poisson-Dirichlet polygon. Finally, they thank two referees for critical comments.

References

[1] Affentranger, F. and Dwyer, R.A., The convex hull of random balls, Adv. in Appl. Probab. **25** (1993), 373–394.

[2] Aldous, D., Fristedt, B., Griffin, Ph.S. and Pruitt, W.E., The number of extreme points in the convex hull of a random sample, J. Appl. Probab. **28** (1991), 287–304.

[3] Bookstein, F.L., *Morphometric Tools for Landmark Data: Geometry and Biology*, Cambridge Univ. Press (1991), Cambridge.

[4] Brozius, H., Convergence in mean of some characteristics of the convex hull, Adv. in Appl. Probab. **21** (1989), 526–542.

[5] Brozius, H. and de Haan. L., On limiting laws for the convex hull of a sample, J. Appl. Probab. **24** (1987), 852–862.

[6] Buchta, C., Zufällige Polyeder: Eine Übersicht, Lect. Notes Math. **1114** (1985), 1–13.

[7] Cabo, A. and Groeneboom, P., Limit theorems for functionals of convex hulls, Probab. Theor. Relat. Fields **100** (1994), 31–55.

[8] Carnal, H., Die konvexe Hülle von n rotationssymmetrisch verteilten Punkten, Z. Wahrsch. verw. Gebiete **15** (1970), 168–179.

[9] Daley, D.J. and Vere-Jones, D., *An Introduction to the Theory of Point Processes*, Springer (1988), New York.

[10] Davis, R.A., Mulrow, E. and Resnick, S.I., The convex hull of a random sample in $\mathbf{R}^2$, Comm. Statist. Stochastic Models **3(1)** (1987), 1–27.

[11] Dwyer, R.A., Convex hulls of samples from spherically symmetric distribution, Discrete Appl. Math. **31** (1991), 113–132.

[12] de Haan, L., Omey, E. and Resnick, S.I., Domains of attraction and regular variation in $\mathbf{R}^d$, J. Multivariate Anal. **14** (1984), 17–33.

[13] Hawkins, A.E., *The Shape of Powder-Particle Outlines*, Research Studies Press, Taunton, Somerset, England and J.Wiley and Sons (1993), New York, Chichester.

[14] Hsing, T., On the asymptotic distribution of the area outside a random convex hull in a disk. Ann. Appl. Probab. **4** (1994), 478–493.

[15] Kendall, D.G., Shape manifolds, procrustean metrics, and complex projective spaces, Bull. London Math. Soc. **16** (1984), 81–121.

[16] Matheron, G., *Random Sets and Integral Geometry*, Wiley (1975), New York.

[17] Miles, R.E., Random polygons determined by random lines in a plane. I, II, Proc. Natl. Acad. Sci. (U.S.A.) **52** (1964), 901–907 and 1157–1160.

[18] Molchanov, I.S., Limit theorems for convex hulls of random sets, Adv. in Appl. Probab. **25** (1993), 395–414.

[19] Molchanov, I.S., *Limit Theorems for Unions of Random Closed Sets*, volume 1561 of *Lect. Notes Math.*, Springer (1993), Berlin.

[20] Okabe, A., Boots, B. and Sugihara, K., *Spatial Tesselations — Concepts and Applications of Voronoi Diagrams*, Wiley (1992), Chichester.

[21] Pirard, E., Roughness analysis on powders using mathematical morphology, Acta Stereologica **11** (Suppl. I) (1992), 533–538.

[22] Pirard, E., Shape processing and analysis using the calypter, J. Microscopy **175** (1994), 214–221.

[23] Rényi, A. and Sulanke, R., Über die konvexe Hülle von n zufällig gewällten Punkten, Z. Wahrsch. verw. Gebiete **2** (1963), 75–84.

[24] Resnick, S.I., *Extreme Values, Regular Variation and Point Processes*, Springer (1987), Berlin.

[25] Schneider, R., Random approximations of convex sets, J. Microscopy **151** (1988), 211–227.

[26] Serra, J., *Image Analysis and Mathematical Morphology*, Academic-Press (1982), London.

[27] Stoyan, D., Kendall, W.S. and Mecke, J., *Stochastic Geometry and Its Applications*, Wiley (1987), Chichester.

[28] Stoyan, D. and Stoyan, H., *Fractals, Random Shapes and Point Fields*, Wiley, Chichester etc., 1994.

[29] Vitale, R.A., Some developments in the theory of random sets, Bull. Inst. Intern. Statist. **50** (1983), 863–871.

Received: 5/2/1994
Revised: 4/20/1995
Accepted: 4/28/1995

Recommended by Richard Cowan, Editor